



PAPER

Analysis of relative changes in pulse shapes of intracranial pressure and cerebral blood flow velocity

OPEN ACCESS

RECEIVED
29 June 2021REVISED
29 October 2021ACCEPTED FOR PUBLICATION
11 November 2021PUBLISHED
29 December 2021

Original content from this work may be used under the terms of the [Creative Commons Attribution 4.0 licence](#).

Any further distribution of this work must maintain attribution to the author(s) and the title of the work, journal citation and DOI.

Arkadiusz Ziółkowski^{1,4} , Agata Pudelko^{1,4} , Agnieszka Kazimierska¹ , Zofia Czosnyka², Marek Czosnyka^{2,3,5} and Magdalena Kasprowicz^{1,5} ¹ Department of Biomedical Engineering, Faculty of Fundamental Problems of Technology, Wrocław University of Science and Technology, Wrocław, Poland² Division of Neurosurgery, Department of Clinical Neurosciences, Addenbrooke's Hospital University of Cambridge, Cambridge, United Kingdom³ Institute of Electronic Systems, Warsaw University of Technology, Poland⁴ These authors contributed equally to this work and share joint first authorship.⁵ These authors share joint senior authorship.E-mail: magdalena.kasprowicz@pwr.edu.pl**Keywords:** intracranial compliance, intracranial pressure, transcranial Doppler, cerebral blood flow, hydrocephalus, morphological analysis**Abstract**

Objective. Analysis of relative changes in the shapes of pulse waveforms of intracranial pressure (ICP) and transcranial Doppler cerebral blood flow velocity (CBFV) may provide information on intracranial compliance. We tested this hypothesis, introducing an index named the ratio of pulse slopes (RPS) that is based on inclinations of the ascending parts of the ICP and CBFV pulse waveforms. It has hypothetically a simple interpretation: a value of 1 indicates good compliance and a value less than 1, reduced compliance. Here, we investigated the usefulness of RPS for assessment of intracranial compliance. **Approach.** ICP and CBFV signals recorded simultaneously in 30 normal-pressure hydrocephalus patients during infusion tests were retrospectively analysed. CBFV was measured in the middle cerebral artery. Changes in RPS during the test were compared with changes in the height ratio of the first and second peak of the ICP pulse (P1/P2) and the shape of the ICP pulse was classified from normal (1) to pathological (4). Values are medians (lower, upper quartiles). **Main results.** There was a significant correlation between baseline RPS and intracranial elasticity ($R = -0.55$, $p = 0.0018$). During the infusion tests, both RPS and P1/P2 decreased with rising ICP [RPS, 0.80 (0.56, 0.92) versus 0.63 (0.44, 0.80), $p = 0.00015$; P1/P2, 0.58 (0.50, 0.91) versus 0.52 (0.36, 0.71), $p = 0.00009$] while the ICP pulses became more pathological in shape [class: 3 (2, 3) versus 3 (3, 4), $p = 0.04$]. The magnitude of the decrease in RPS during infusion was inversely correlated with baseline P1/P2 ($R = -0.40$, $p < 0.03$). **Significance.** During infusion, the slopes of the ascending parts of ICP and CBFV pulses become increasingly divergent with a shift in opposite directions. RPS seems to be a promising methodological tool for monitoring intracranial compliance with no additional volumetric manipulation required.

1. Introduction

The shape of the intracranial pressure (ICP) pulse waveform is determined by pulsatile cerebral arterial inflow, cerebral venous outflow and the mechanoelastic properties of the cerebrospinal fluid (CSF) space (Balédent *et al* 2004). The ICP pulse generally has three characteristic peaks, referred to as P1 (percussion wave), P2 (tidal wave) and P3 (dicrotic wave), with a valley between P2 and P3 termed the dicrotic notch (denoted N) (Cardoso *et al* 1983). In normal conditions, P1 is higher than both P2 and P3 and the notch is visible. Under pathophysiological conditions, with rise in mean ICP, initially the amplitudes of the first two peaks (P1 and P2) increase, then P2 becomes predominant and the dicrotic notch gradually disappears. Finally, all peaks become indistinguishable and the shape of the ICP pulse becomes rounded or triangular (Fan *et al* 2008).

Rounding of the pulse waveform is often observed at elevated ICP and the morphological changes have been associated with changes in mean ICP for a long time (Chopp and Portnoy 1980, Contant Jr *et al* 1995). However, the results of a recent study demonstrated that the transition to ‘rounded’ morphology varies over time and across patients and is not solely dependent on mean ICP (Ellis *et al* 2006). Decreased intracranial compliance (C_i), i.e. reduced ability of the system to tolerate or compensate for volume increases, has also been reported as a potential cause of the alterations in the shape of the ICP pulse waveform (Heldt *et al* 2019). A decrease in C_i may predate an increase in mean ICP; therefore, monitoring of C_i can often be more clinically useful than monitoring of the ICP level alone.

Traditionally, estimation of C_i requires external volumetric manipulation, such as addition or removal of fluid from the craniospinal space, to assess the pressure response to a given change in volume (Heldt *et al* 2019). As a result, the procedure is additionally invasive and may not be applicable to some clinical scenarios such as brain trauma. To overcome that limitation, many attempts have been made to assess C_i based on analysis and interpretation of ICP pulse morphology (Germon 1988, Robertson *et al* 1989, Berdyga *et al* 1993, Fan *et al* 2008, Hu *et al* 2008). The ratio of the heights of the first and second peaks of the ICP pulse waveform (P1/P2 ratio) was suggested as a measure of C_i in the 1980s (Cardoso *et al* 1983), and its good correlation with the direct method of volumetric manipulation was recently confirmed by Kazimierska *et al* (2021). Morphological classification of ICP pulses using an artificial neural network was shown to be a useful diagnostic tool for identification of patients with altered CSF hydrodynamics prior to volume infusion (Nucci *et al* 2016). Only one study has analysed the relationship between pulse ICP and pulse cerebral blood flow velocity (CBFV) measured in the middle cerebral artery with transcranial Doppler (TCD) ultrasonography using the spectral phase shift between the signals (Kim *et al* 2015). However, the relative changes in ICP and CBFV pulse shapes, in particular during increase in mean ICP, have not yet been investigated in detail and compared with other ICP pulse shape-derived indices of C_i .

Therefore, we aim to further analyse the relationship between pulse ICP and CBFV before and during controlled elevation of mean ICP induced by the infusion test. Our goal is threefold. The first is to introduce an index for intracranial compliance assessment that is calculated in the time domain based on slopes of the ascending parts of the ICP and CBFV pulse waveforms. We named this the ratio of pulse slopes (RPS). The second aim is to compare changes in the RPS before and during the infusion test with changes in other ICP pulse shape-derived indices of C_i such as the morphological class of ICP pulse shape and the P1/P2 ratio. Finally, we aim to compare RPS with conventional indices used clinically for the assessment of the state of intracranial compensatory mechanisms in hydrocephalus patients: intracranial elasticity (E), which is an index inversely related to C_i , and the index of compensatory reserve (RAP).

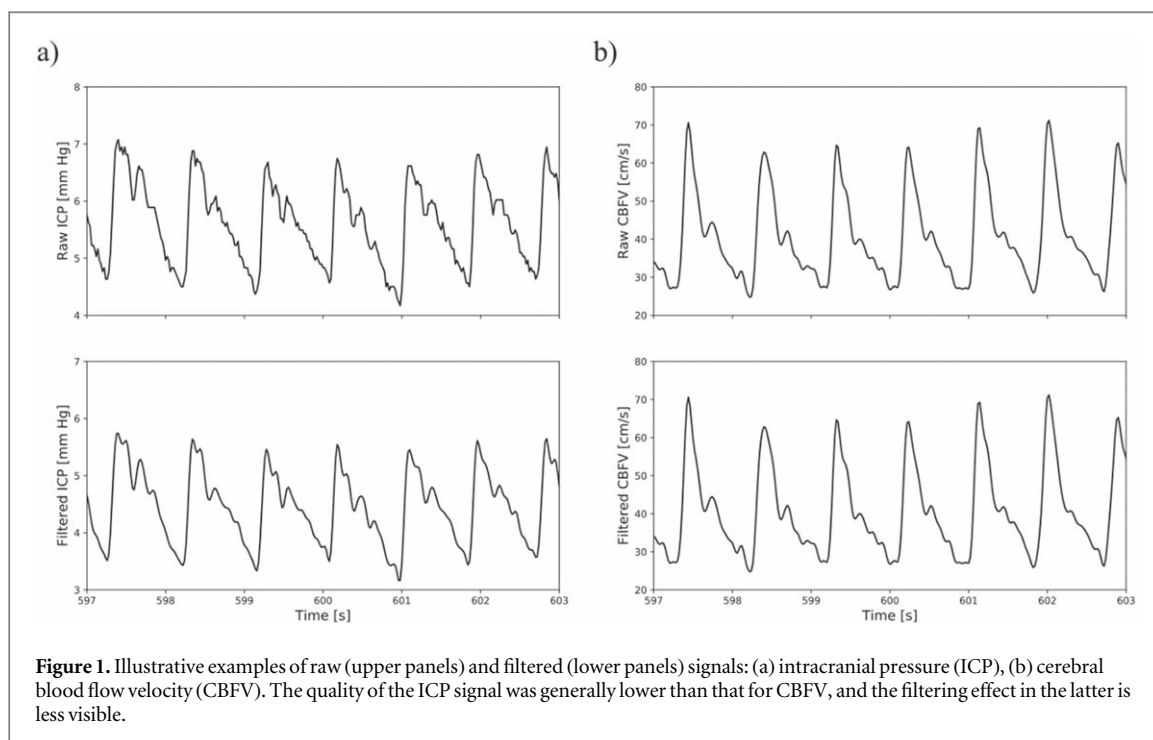
The proposed index may have clinical applicability in continuous intracranial compliance monitoring, which in turn could help predict dangerous increases in ICP. Our goal was to develop a methodology that does not require the manipulation of intracranial volume and therefore can be used in patients in whom changes in intracranial volume could be life-threatening (e.g. in traumatic brain injury or subarachnoid haemorrhage), that is easy to understand, does not require peak identification (unlike the P1/P2 ratio) or complex machine learning algorithms (unlike pulse shape classification) and, due to simultaneous analysis of two physiological signals, may provide additional information about the cerebrospinal dynamics.

2. Materials and methods

2.1. Patient cohort and data acquisition

Recordings from 30 non-shunted normal-pressure hydrocephalus (NPH) patients were selected from a database of 51 patients who underwent constant-rate infusion tests at Addenbrooke’s Hospital (Cambridge, UK) between 1992 and 2000 with simultaneous recording of ICP and CBFV. The primary criterion for selection was good-quality ICP and CBFV signals sufficient to analyse the pulse waveforms in the time domain. The initial dataset was not collected with the explicit purpose of analysing the ICP and CBFV pulse waveform in detail, which led to a relatively high percentage of cases excluded on the basis of low signal quality. Sixteen out of 21 rejected recordings were excluded due to unfeasibility of peak designation in the ICP pulse contour caused by a low signal-to-noise ratio. The next five registrations were rejected due to poor CBFV signal quality. In total, 62 831 pulse waveforms of each signal (78.3% of all pulses recorded in all 30 patients) were included in analysis. The rest of the pulses were excluded due to low quality or local distortions, as described in the sections below.

In all patients the infusion test was performed based on the methodology introduced by Katzman and Hussey (1970). The standard clinical procedure of the infusion test for NPH patients was extended with the CBFV measurement, with the approval from the local ethical committee (no. 08/H0306/103). In short, ICP and CBFV signals were recorded simultaneously during constant-rate infusion of normal saline into the CSF space (1.5 ml min^{-1} in patients with normal baseline pressure or 1.0 ml min^{-1} if the baseline pressure was greater than



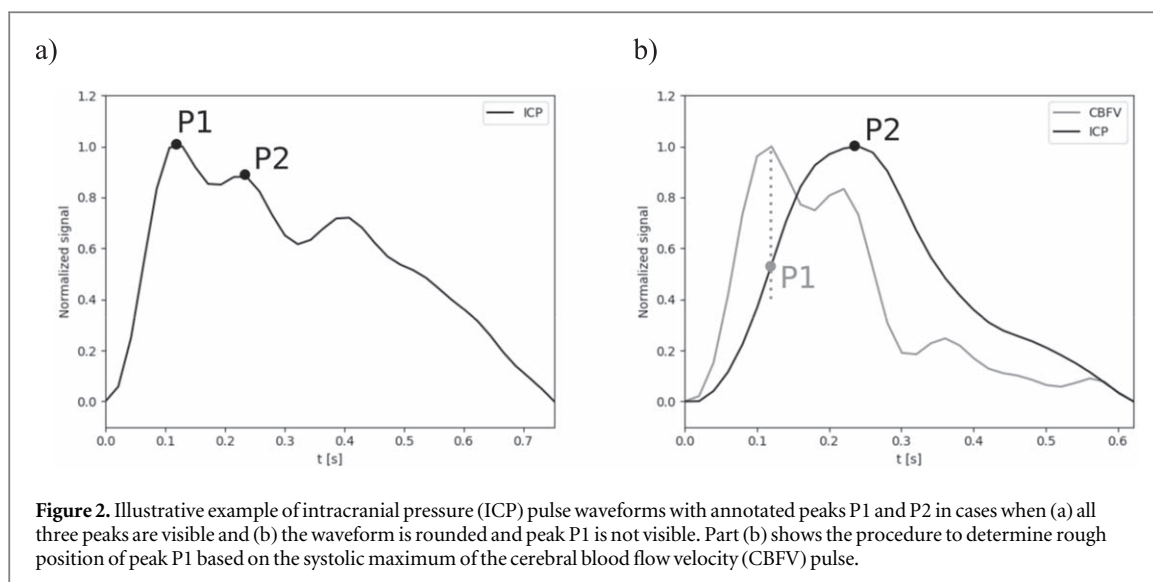
15 mmHg; Czosnyka *et al* 1996). ICP was measured using a hypodermic needle (25 gauge) inserted into a pre-implanted Ommaya reservoir and connected to a pressure transducer via a saline-filled tube. A second needle was used for infusion. CBFV in the middle cerebral artery was monitored using a TCD system (Neuroguard, Medasonics, Fremont, CA, USA) with a 2 MHz probe. The signals were recorded using custom software for waveform collection (WREC, W. Zabolotny, Warsaw University of Technology, Warsaw, Poland). After 10 min of baseline recording, the infusion was started. The constant-rate infusion (1.5 ml min^{-1} or 1.0 ml min^{-1}) was continued until a steady state of ICP was achieved (plateau phase) or stopped when ICP increased above the safety limit of 40 mmHg. The anonymized recordings of ICP and CBFV were retrospectively analysed as part of routine clinical audit. To keep the research procedure consistent, only right-side CBFV was used as all patients had good-quality recordings on that side.

2.2. CSF compensatory parameters

In order to derive indices describing CSF dynamics, infusion test recordings of the ICP signal were processed using specialized software (ICM+, Cambridge Enterprise, Cambridge, UK). Three parameters were calculated: intracranial elasticity (E), resistance to CSF outflow (R_{out}) and the RAP index. E is a parameter which in theory describes the stiffness of the brain in relation to displacement of cerebral blood volume and is inversely related to C_i . Elevation of E above 0.18 ml^{-1} indicates diminished pressure–volume compensatory reserve (Marmarou *et al* 1996). R_{out} represents CSF outflow capacity and is used as a potential predictor of the outcome of shunting in hydrocephalus (Tans and Boon 2002): $R_{\text{out}} > 13 \text{ mmHg ml}^{-1} \text{ min}^{-1}$ in younger adults (Børgesen and Gjerris 1982) or $18 \text{ mmHg ml}^{-1} \text{ min}^{-1}$ in the elderly indicates disturbed CSF outflow (Boon *et al* 1997). Both parameters (E and R_{out}) were calculated based on Marmarou's model of cerebrospinal dynamics (Marmarou *et al* 1978) using the built-in analysis module of ICM+ (Smielewski *et al* 2012). RAP (described in detail in Czosnyka *et al* (1988)) is an index of cerebrospinal compensatory reserve and indicates the degree of correlation between the amplitude of the fundamental component of ICP pulse and mean ICP over short periods of time (calculation window 5 min, shifted every 10 s). A value of RAP close to +1 denotes that the compensatory reserve is low.

2.3. ICP pulse shape-derived indices of intracranial compliance

Prior to pulse shape analysis, both ICP and CBFV signals were processed using a low-pass filter with a cut-off frequency of 10 Hz to remove high-frequency noise, primarily from the ICP signal (a comparison of raw and filtered signals is presented in figure 1). Detection of individual pulses was performed using the modified Scholkmann algorithm (Bishop and Ercole 2018). In addition to the indices described below, each ICP pulse was also characterized by its amplitude (AMP ICP) calculated as the peak-to-peak value between minimum and maximum ICP in the pulse (the same procedure was independently applied to CBFV pulses to obtain AMP CBFV). All analyses were carried out using programs custom-written in Python.



2.3.1. P1/P2 ratio

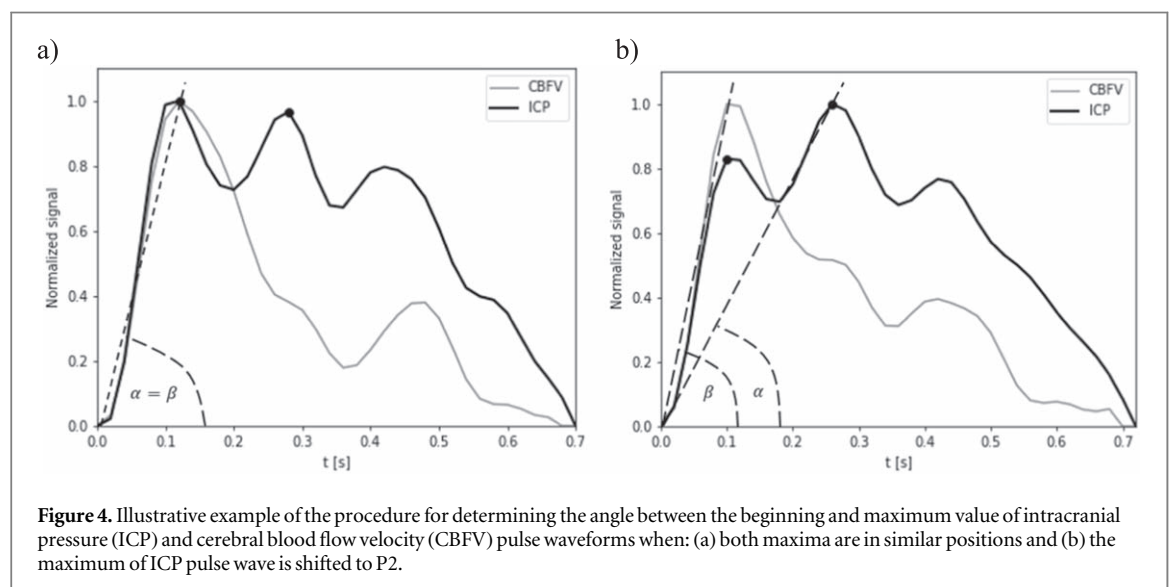
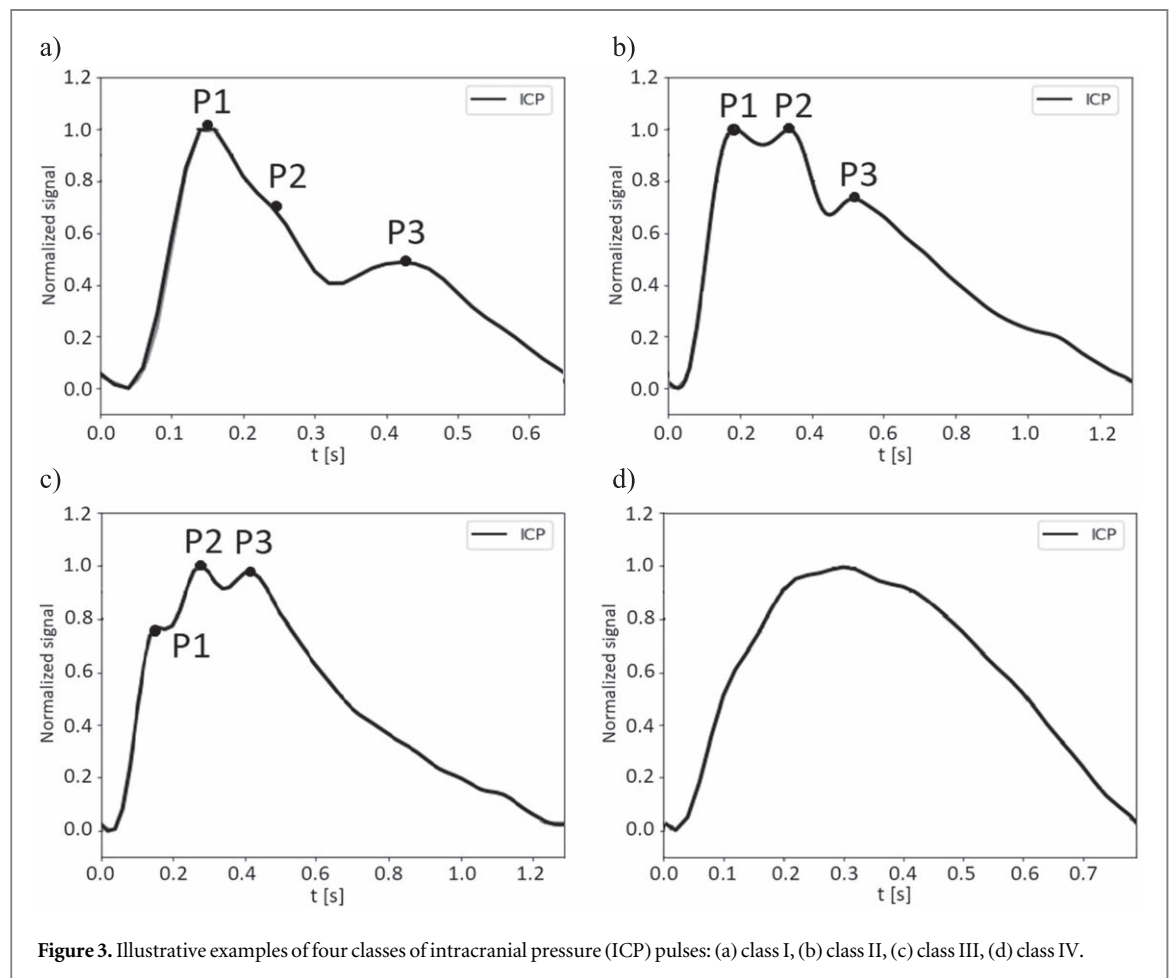
The height ratio of the first and second peak of the ICP pulse waveform was assessed based on manual annotation of P1 and P2 positions performed by an expert researcher in every pulse. First, ICP and CBFV pulses were aligned with regard to the pulse onset point in order to remove the time delay caused by the distance between measurement sites. Pulses with distorted waveforms (e.g. containing short-term disturbances or non-physiological peaks resulting from artefacts at the signal collection stage) were marked based on the researcher's experience and examples of valid and invalid pulses available in the literature (Cardoso *et al* 1983, Carrera *et al* 2010, Meghani *et al* 2019) and excluded from further analysis. Next, peak height was calculated as the vertical distance between the peak and the pulse onset point. An illustrative example of an ICP pulse waveform with peak annotations is presented in figure 2(a). In rounded pulses with indistinguishable P1 the rough P1 position was estimated based on the location of the systolic maximum of the CBFV signal in order to enable comparison between the P1/P2 ratio and other indices in the same number of waveforms (figure 2(b)). The median error of this method of P1 height assessment was estimated as 0.15% [−2.83% to 5.86%] based on comparison between manually annotated P1 and positions derived from the CBFV pulses in 2388 randomly selected pulses where the peaks are normally visible (see figures 3(a)–(c)).

2.3.2. Morphological classification

Classification of ICP pulse shapes was based on the method proposed in Nucci *et al* (2016) which takes into account the overall shape of the waveform in terms of relative height and visibility of characteristic peaks but does not require peak detection. In this work, ICP pulse shapes were classified manually by an expert researcher; however, this task can be automated using machine learning algorithms, as shown in the original paper and more recently in Mataczynski *et al* (2021). The following classes were identified: (a) class I, where all three peaks (P1, P2, P3) are visible and the height of P1 exceeds the heights of P2 and P3; (b) class II, where all three peaks are visible, and the heights of P1 and P2 are similar or P2 dominates over P1, but P1 dominates over P3; (c) class III, where all three peaks are visible and the heights of both P2 and P3 exceed the height of P1; (d) class IV, where the pulse shape is so rounded that it contains only one clear maximum and the three peaks cannot be distinguished. These criteria are visualized in figure 3. Based on the classification of individual pulses, each recording was characterized by its dominant class, defined as the class which describes the majority of pulses in the selected time period (at baseline and during the plateau phase of the test).

2.3.3. Ratio of pulse slopes

The RPS was estimated based on the slopes of the ascending parts of ICP and CBFV pulse waveforms. The ascending part was defined at the portion of the signal from pulse onset point to maximum of the pulse contour. First, the cosine value of the angle between the maximum of each pulse waveform and its beginning was calculated. Note that in this case no additional pre-processing such as alignment of ICP and CBFV pulse onsets was required. Next, RPS was determined as the quotient of the cosine value of CBFV and ICP pulses, described as:



$$RPS = \frac{\cos(\beta_{CBFV})}{\cos(\alpha_{ICP})} \tag{1}$$

The RPS depends strictly on the position of the maximum in each pulse waveform (see figure 4).

If the maximum of the ICP pulse is located on the time axis at a position similar to the maximum of CBFV (i.e. P1 is the dominant peak), the slopes are also similar and RPS is close to 1. As the maximum of the ICP pulse

wave is shifted to P2 or P3 while the location of the systolic peak of the CBFV pulse remains unchanged or is slightly moved towards the onset of the pulse with rising ICP, RPS decreases below 1.

2.4. Statistical analysis

Non-parametric tests were used for statistical analyses (assumption of normality was rejected by the Shapiro–Wilk test for the majority of variables). The relationships between CSF compensatory parameters and the ICP pulse shape-derived indices were assessed using Spearman rank correlation coefficient (R_{Spearman}). The Wilcoxon signed-rank test was used to compare median values of analysed parameters at baseline and during the plateau phase of the infusion test. The level of significance was set at 0.05. All statistical analyses were performed with Statistica 13.1 (Tibco, Palo Alto, CA, USA) software.

3. Results

The subjects comprised 16 men and 14 women with a median age 58 years [interquartile range (IQR) 36–67 years]. Ventricular dilation was diagnosed by a clinician based on the bicaudate index (BCI) and the width of the third ventricle. According to age-dependent thresholds for BCI (Little *et al* 2008) and third ventricle width (Meese *et al* 1980), every patient enrolled in this study had an increased BCI (median 0.28, IQR 0.19–0.34) and width of the third ventricle (median 13.06 mm, IQR 9.98–16.65 mm), which implied ventricular dilatation. Based on the presence of infarcts and deep white matter lesions in cranial imaging, an independent neurologist found evidence of ischaemia in seven patients. No patients presented signs of aqueductal stenosis.

An illustrative example of changes in physiological signals and derived indices over the course of the infusion test is presented in figure 5.

Median values and lower and upper quartiles of compensatory parameters E , R_{out} and RAP are given in table 1. Changes in analysed parameters between baseline and the plateau phase of the test are provided in table 2. The median RAP at baseline was elevated, suggesting reduced CSF compensatory reserve in the study cohort. Baseline ICP pulse waves were pathological in shape, and both the P1/P2 ratio and RPS were reduced at baseline, indicating diminished intracranial compliance.

All shape-derived parameters calculated at baseline (RPS, P1/P2 ratio, and dominant class of ICP pulse shape) were significantly correlated with E , with the strongest correlation observed between RPS and E (see figures 6(a)–(c)). There was also significant correlation between baseline RAP and E (figure 6(d)). Baseline RAP was correlated with the P1/P2 ratio and RPS (see figures 7(a), (b)) but the association with dominant ICP pulse class was on the border of statistical significance ($R_{\text{Spearman}} = 0.34$, $p = 0.064$). No significant correlations were found between any of the ICP pulse shape-related parameters (P1/P2 ratio, ICP pulse class and RPS) and either R_{out} , mean ICP, mean CBFV, pulse amplitude of ICP or pulse amplitude of CBFV at baseline. There were also no statistically significant correlations between median values of shape-derived parameters calculated during plateau phase (P1/P2 ratio, ICP dominant pulse class and RPS) and cerebrospinal compensatory parameters (E and R_{out}).

During the infusion test, both the RPS and the P1/P2 ratio decreased. The median value of the dominant class of pulse ICP shape remained unchanged, but the IQR was shifted towards higher values (see table 2 for detailed results of baseline versus plateau phase analysis). The magnitude of decrease in RPS during infusion was inversely correlated with the P1/P2 ratio at baseline (figure 8). It was also positively correlated with the class of ICP pulse shape at baseline, although this relationship was statistically insignificant ($R_{\text{Spearman}} = 0.33$, $p = 0.075$). The degree of change in RPS between baseline and the plateau phase was not correlated with either baseline ICP, AMP ICP, AMP CBFV, RAP or E .

4. Discussion

In this study we analysed changes in the slopes of the ascending parts of pulse ICP and CBFV waveforms and showed that the ratio of these slopes (or, more precisely, the ratio of the cosines of the slope angle of CBFV and ICP pulse waves) decreases with rising ICP during infusion. The magnitude of this decrease depends on the baseline shape of the ICP pulse, which means that a normal or slightly pathological shape (P1/P2 ratio greater than or a little less than 1) at baseline is associated with larger drop in RPS during infusion. Finally, we found significant correlation between baseline RPS and intracranial elasticity, suggesting usefulness of proposed index for assessment of intracranial compliance without the need for volumetric manipulation.

Analysis of the P1/P2 ratio showed a significant drop during controlled rise of ICP performed in hydrocephalus patients (Kazimierska *et al* 2021). Morphologically classified shapes of pulse ICP waveforms changes towards more pathological patterns during elevation of ICP induced by infusion, as shown in Elixmann *et al* (2012) and Nucci *et al* (2016). As in our study, Kazimierska *et al* (2021) observed the largest changes in

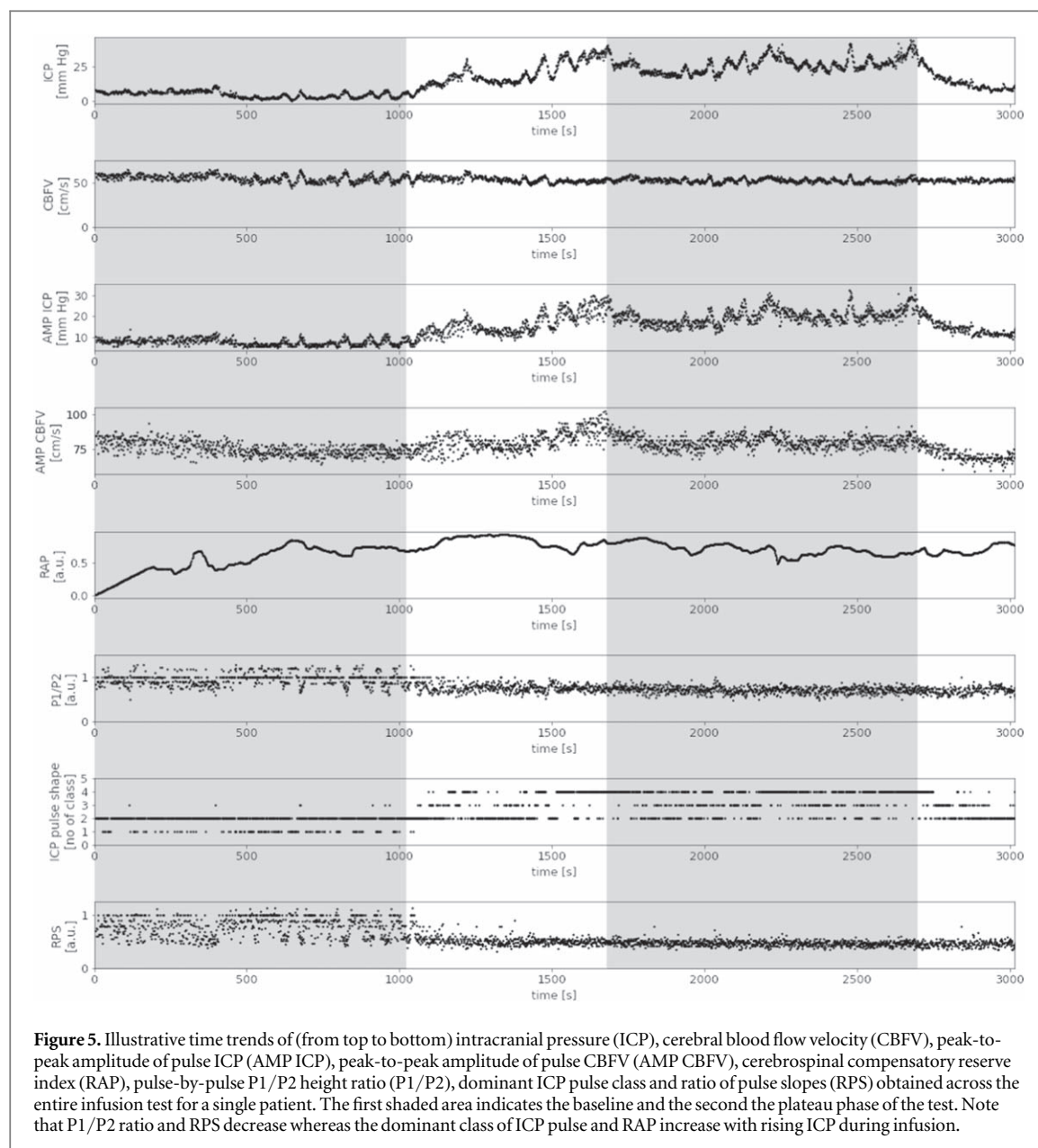


Figure 5. Illustrative time trends of (from top to bottom) intracranial pressure (ICP), cerebral blood flow velocity (CBFV), peak-to-peak amplitude of pulse ICP (AMP ICP), peak-to-peak amplitude of pulse CBFV (AMP CBFV), cerebrospinal compensatory reserve index (RAP), pulse-by-pulse P1/P2 height ratio (P1/P2), dominant ICP pulse class and ratio of pulse slopes (RPS) obtained across the entire infusion test for a single patient. The first shaded area indicates the baseline and the second the plateau phase of the test. Note that P1/P2 ratio and RPS decrease whereas the dominant class of ICP pulse and RAP increase with rising ICP during infusion.

Table 1. Cerebrospinal fluid (CSF) compensatory parameters. Medians and quartiles were calculated from all 30 infusion tests.

| Parameters | Median | Low Q | High Q |
|--|--------|-------|--------|
| E (ml^{-1}) | 0.17 | 0.13 | 0.25 |
| R_{out} ($\text{mmHg ml}^{-1} \text{min}^{-1}$) | 12.2 | 9.0 | 14.4 |
| RAP index at baseline (a.u.) | 0.62 | 0.39 | 0.75 |

E , intracranial elasticity; R_{out} , resistance to CSF outflow; RAP, cerebrospinal compensatory reserve index; a.u., arbitrary units. E and R_{out} were calculated from the whole infusion test recording using Marmarou's model (Marmarou *et al* 1978) of CSF dynamics.

P1/P2 ratio during the infusion phase of the test in cases where baseline ICP waveform contained P1 dominating over P2 (which means that the shape of ICP pulse wave was normal). A possible explanation for that observation might be as follows. In patients with a normal shape of the ICP pulse waveform the ability to compensate volumetric changes is likely preserved (the CSF system is highly compliant). Therefore, a wide spectrum of morphological changes in the ICP pulse wave, and consequently in RPS, can be seen during a gradual rise in mean ICP caused by infusion. In contrast, in patients demonstrating a pathological shape of the ICP pulse wave

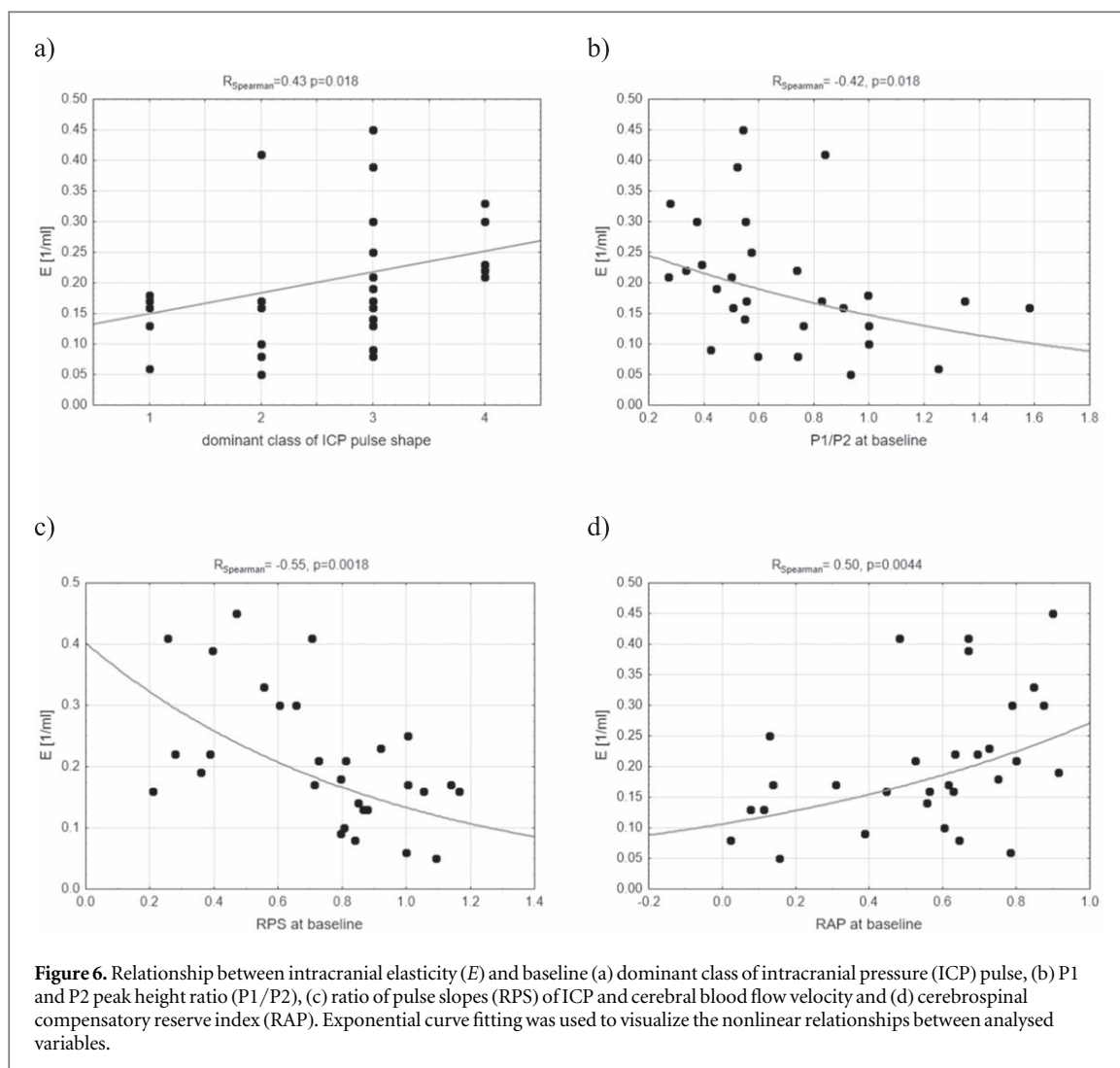


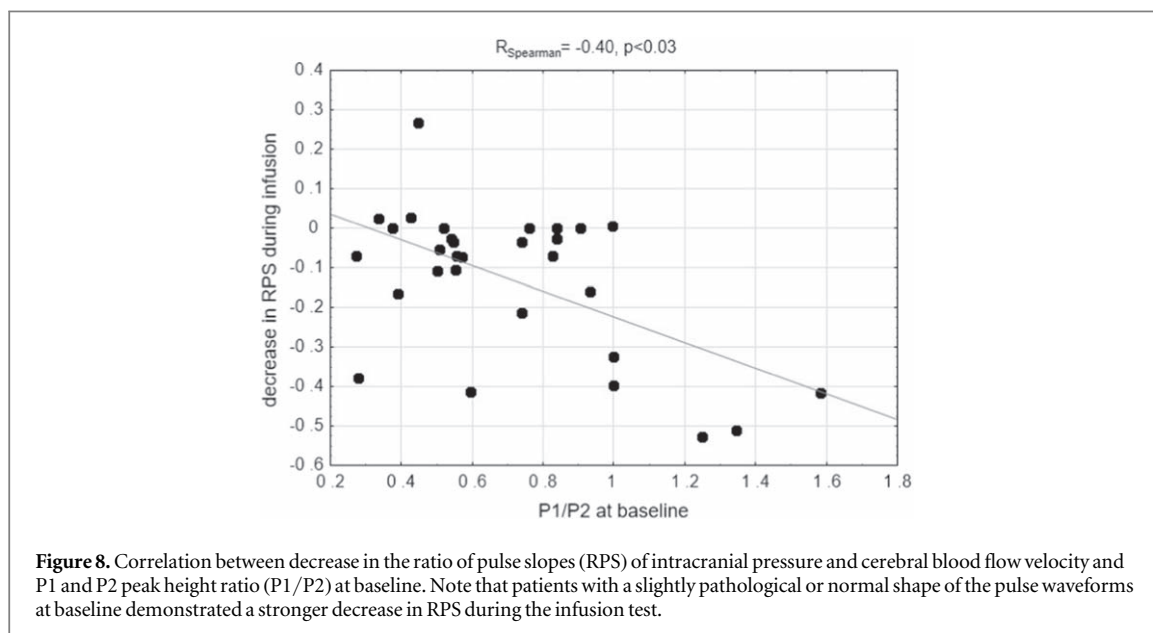
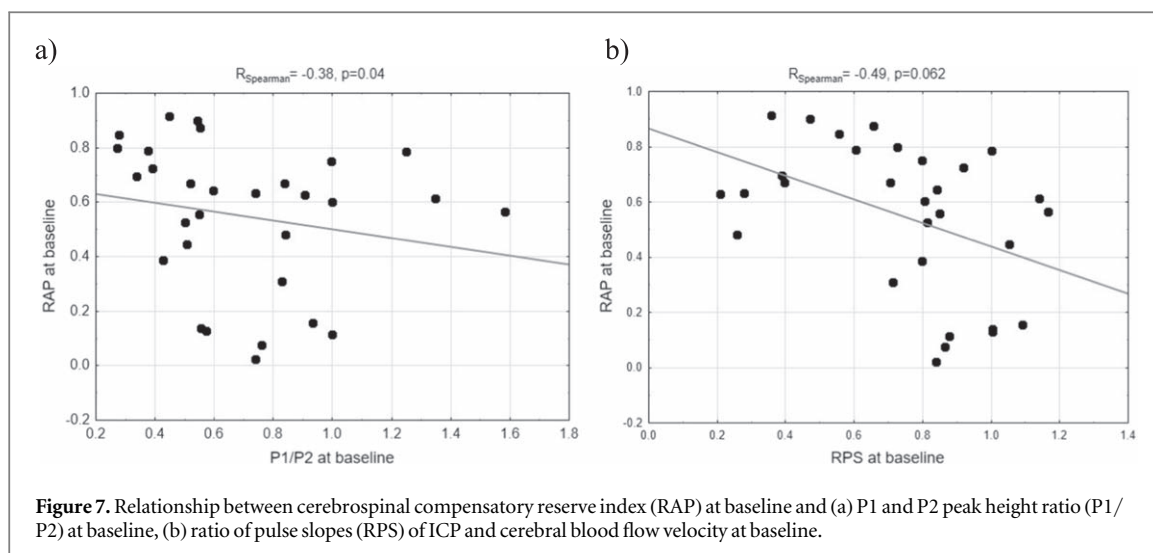
Figure 6. Relationship between intracranial elasticity (E) and baseline (a) dominant class of intracranial pressure (ICP) pulse, (b) P1 and P2 peak height ratio (P1/P2), (c) ratio of pulse slopes (RPS) of ICP and cerebral blood flow velocity and (d) cerebrospinal compensatory reserve index (RAP). Exponential curve fitting was used to visualize the nonlinear relationships between analysed variables.

Table 2. Median values (lower quartile, upper quartile) of physiological signals and calculated variables at baseline and during the plateau phase of the test.

| Parameters | Baseline | Plateau | p -value |
|---------------------------------|----------------------|----------------------|------------|
| ICP (mmHg) | 9.15 (6.40, 12.34) | 21.7(17.6, 26.9) | 0.000 002 |
| CBFV (cm s^{-1}) | 51.5 (40.3, 59.7) | 47.7 (36.5, 60.6) | 0.000 058 |
| AMP ICP (mmHg) | 3.54 (2.31, 4.60) | 7.4 (5.8, 11.5) | 0.000 002 |
| AMP CBFV (cm s^{-1}) | 41.31 (35.96, 53.86) | 41.68 (35.29, 53.98) | 0.011 |
| RAP (a.u.) | 0.62 (0.39, 0.75) | 0.74 (0.66, 0.82) | 0.033 |
| ICP pulse dominant class (a.u.) | 3(2, 3) | 3 (3, 4) | 0.04 |
| P1/P2 (a.u.) | 0.58 (0.50, 0.91) | 0.52 (0.36, 0.71) | 0.000 09 |
| RPS (a.u.) | 0.80 (0.56, 0.92) | 0.63 (0.44, 0.80) | 0.000 15 |

ICP, intracranial pressure; CBFV, cerebral blood flow velocity; AMP ICP, peak-to-peak amplitude of pulse ICP; AMP CBFV, peak-to-peak amplitude of pulse CBFV; RAP, cerebrospinal compensatory reserve index; P1/P2, pulse-by-pulse P1/P2 height ratio; RPS, ratio of pulse slopes; a.u., arbitrary units; p -value, probability level of Wilcoxon signed-rank test.

at baseline the compensatory mechanisms are diminished and further modification of ICP pulse shape with rising ICP is limited. This is reflected by a small (or absent) decrease or even a slight increase in RPS during infusion. Interestingly, baseline RPS does not correlate with baseline mean ICP. No association with baseline ICP was found for the P1/P2 ratio either (neither in our study nor in Kazimierska *et al* (2021)) or for pulse phase shift (Kim *et al* 2015). This supports the hypothesis that reduction in intracranial compliance may occur independently of the mean ICP level. However, all analysed parameters estimated at baseline (RPS, P1/P2 ratio and morphological class of ICP pulse shape) were associated with intracranial elasticity. It is worth noting that



estimation of E requires the introduction of external volumetric change whereas analysis of RPS and ICP pulse morphology is not additionally invasive.

The accordance of our findings with previously published results confirms the ability of RPS to assess the state of CSF dynamics. The novel aspect introduced in our study is the simple, time-domain index for estimation of intracranial compliance. Previous research (Kim *et al* 2015) focused on the spectral phase shift between ICP and CBFV. Spectral analysis based on the Fourier transform is historically the first signal processing technique that was used to investigate changes in the ICP pulse waveform (Portnoy and Chopp 1981, Czosnyka *et al* 1988, Christensen and Børgesen 1989, Robertson *et al* 1989, Berdyga *et al* 1993). However, under clinical conditions, with frequent sudden changes in pressure or cardiac arrhythmia, the signal stationarity requirements of the Fourier transform are often not met. Moreover, the transmission from CBFV to ICP pulse is most likely nonlinear (the pulse amplitudes of ICP and CBFV signals show a nonlinear relationship during the increase in ICP induced by infusion; based on in-house research results, unpublished data), making spectral analysis imprecise for processing of these signals. Therefore, the spectral approach may lead to unreliable results for pulse phase shift estimation. RPS as a time-domain index is not burdened by this limitation. The proposed methodology provides a relative measure that reflects how the ICP pulse waveform differs from the normal shape without performing advanced morphological analysis. Moreover, examination of the relationship between two signals rather than absolute changes in individual slopes has the advantage of providing reference values and allowing the results to be presented in an easy to interpret linear scale. At normal compliance, with P1 as the dominant peak, the maximum of the ICP pulse contour correlates with the systolic peak of CBFV and the

slopes are similar (RPS is close to 1). As intracranial compliance decreases and P2 starts to rise above P1, the maximum moves towards the latter portion of the ICP waveform. The shape of the CBFV pulse also changes in various haemodynamic conditions (Plougmann *et al* 1994, Aggarwal *et al* 2008, de Riva *et al* 2012, Lawley *et al* 2019, Khan and Wiersema 2020, Thorpe *et al* 2020). With rising ICP during infusion, the slope of CBFV pulse slightly increases (which is due to increase in the CBFV pulse amplitude) while the slope of ICP decreases due to changes in the pulse shape. Therefore, the ascending slopes of ICP and CBFV become increasingly divergent (RPS is lower than 1). Finally, in contrast to the previous study (Kim *et al* 2015), we performed comparative analysis with metrics based solely on the ICP signal, namely the P1/P2 ratio and ICP pulse class, and the results show that RPS exhibits the strongest correlation with intracranial elasticity among the analysed indices.

Analysis of the P1/P2 ratio, although it is a very interesting method for intracranial compliance studies, requires high-quality signals and advanced computational algorithms to precisely identify peaks in the ICP pulse contour. Moreover, this approach fails in the case of invisible P1 or a round-shaped ICP pulse. In our study, when the first peak of the ICP pulse was difficult to designate, P1 was denoted based on the location of the first peak in the CBFV pulse wave. This solution gives only rough information about peak position and was used in our study to enable comparative analysis of the P1/P2 ratio with both RPS and morphological class of ICP pulse shapes on exactly the same number of pulses. Morphological classification of ICP pulse waveform shapes is also based on complex algorithms and machine learning techniques (Elixmann *et al* 2012, Nucci *et al* 2016). Incorporation of new computational methods in medicine is in line with the general advancement in the field of biomedical signal processing and is not a limitation by itself, although the complexity of these methods may restrict their acceptance in the medical community and delay introduction into clinical practice. However, the limitation of the morphological shape classification is its scale narrowed down to 4 (or 5; Elixmann *et al* 2012) general categories. Consequently, many similar shapes of ICP pulse waveform fall within one morphological class. Although the pulses are alike in terms of overall configuration of peaks and notches, the height of their peaks or the slope of the ascending part of the pulse waveform may be slightly different. Such a coarse classification may not be sensitive enough to capture subtle differences. A new, extended classification with additional classes of ICP pulse waveform shapes would probably be required for more accurate assessment of changes in intracranial compliance. A limitation of this method is also reflected in weak or no correlation between baseline dominant class of ICP pulse shape and both E and RAP at baseline.

On the other hand, RPS shows the strongest associations with CSF compensatory indices among the analysed pulse shape-related parameters. It has a simple interpretation (values close to 1 denote good compliance whereas values approaching 0 denote low compliance); its assessment does not require advanced, complex computational methods; it allows for continuous estimation of C_i in real time; and it can be easily implemented in computer-based monitoring systems. RPS represents a method free of any additional risks to the patient as it is not additionally invasive. In most clinical settings, ICP and CBFV are often monitored simultaneously and in a continuous way, especially in patients in whom the assessment of cerebral autoregulation and intracranial compliance is indicated.

5. Limitations

The study was performed with a small number of patients, and the sample size was strictly influenced by case selection requirements. Only adult patients with NPH symptoms and with pre-implanted Ommaya reservoirs were enrolled in the study to ensure that the ICP and CBFV measurement sites were located as close as possible and the time delay between the pulses (resulting from the difference in the place of measurement) was minimal. Moreover, the configuration of peaks in the ICP waveform, and thus its shape and the slope of the ascending part, may differ depending on the site of measurement of the ICP signal. For this reason, we did not analyse patients in whom the infusion test was performed via lumbar puncture. As lumbar puncture is the primary approach in infusion studies, the requirement for a pre-implanted Ommaya reservoir significantly reduced the number of eligible patients. Additionally, TCD measurement is not part of routine clinical investigation in NPH patients, and in some patients CBFV measurement was not feasible due to an insufficient acoustic temporal bone window (Purkayastha and Sorond 2012), which further reduced the number of available recordings. Due to the retrospective nature of the analysis, it was not possible to further increase the sample size. However, the database selected for this study is a unique set of infusion test recordings with simultaneous CBFV recordings, and not using it in favour of a new database could be considered a waste of time, money and resources given the aim of this analysis.

Specifically, the primary aim of our study was to find out if there are relationships between CSF compensatory parameters and the ICP pulse shape-derived indices using the Spearman rank correlation coefficient. Based on our results, we found that there are such relationships, and the value of $|R_{\text{Spearman}}|$ ranged from 0.38 to 0.55 depending on the correlation tested. Our most important conclusion is the existence of a relationship between RPS and E ($R_{\text{Spearman}} = -0.55, p = 0.0018$). A sample of 30 is enough to achieve 80%

power to detect $R_{\text{Spearman}} = 0.5$ using a two-tailed test of $H_0: \rho_s = 0$ with a significance level of 0.05 (May and Looney 2020). In this study we chose to focus on a homogeneous population, therefore a small sample size was sufficient to reflect the correlation. However, in a prospective study, a priori calculated sample size should be larger than 30 to detect R_{Spearman} lower than 0.5, and the results of the study should be regarded as preliminary and repeated on a larger sample size of prospectively collected data.

Another limitation is that we did not routinely monitor potential changes in end-tidal carbon dioxide (EtCO₂) during the infusion study. Change in EtCO₂ would lead to changes in cerebral blood volume and subsequent vasogenic changes in ICP, seen not as vasocycling (B waves) but rather a trend drift of ICP, on top of the response to infusion. This would certainly disturb a monoexponential shape of the pressure–volume curve. Such changes were not present in our recordings. However, alterations in cerebrovascular tone activated by changes in EtCO₂ may have an impact on the results of the infusion test (Czosnyka *et al* 1999), therefore in further study it should be monitored and kept as stable as possible.

Additionally, there is one technical consideration. In order to reduce the divergence in ICP peak annotations, all ICP signals were marked by a single experienced researcher, and the ICP pulse shape classification was performed manually (unlike previous studies using machine learning methods). Such methodology may have introduced operator bias resulting from the annotator's experience.

6. Conclusions

The ratio of the slopes of ascending parts of pulse ICP and CBFV waveforms is related to intracranial elasticity in NPH patients. Results of this study show that RPS may be a promising methodological tool to monitor brain elastic properties with no additional volumetric manipulation required. In addition to hydrocephalus, this technique could also be applicable to other groups where CBFV and ICP are routinely monitored, such as after traumatic brain injury or subarachnoid haemorrhage. Further research is needed to investigate whether RPS is related to treatment outcomes in NPH patients and whether the proposed methodology can be applied to a wider group of neurological disorders.

Acknowledgments

MK was supported by the National Science Centre, Poland (grant no. UMO-2019/35/B/ST7/00500). AK acknowledged the support of the Polish National Agency for Academic Exchange under the International Academic Partnerships program. MC and ZC were supported by Revert Project, Interreg France (Channel Manche) England, funded by ERDF.

Elements of this work were presented at the 13th Annual 2021 Meeting of the Hydrocephalus Society (The International Society for Hydrocephalus and Cerebrospinal Fluid Disorders), 10–13 September 2021, Gothenburg, Sweden (virtual).

Conflict of interest

MC has financial interest in the licensing fee of ICM+ software used for recording and analysis of infusion tests. The other authors have nothing to disclose.

Ethical statement

The data were collected as part of routine clinical investigation following diagnosis of normal-pressure hydrocephalus. Patients gave their consent and anonymized digital recordings of monitored signals were post-processed as part of routine clinical (ID 4012) audit. Additional non-invasive TCD monitoring during the test was approved by the ethics committee (08/H0306/103). The study was conducted in accordance with the principles embodied in the Declaration of Helsinki.

ORCID iDs

Arkadiusz Ziółkowski  <https://orcid.org/0000-0002-2630-514X>

Agata Pudełko  <https://orcid.org/0000-0001-7692-6422>

Agnieszka Kazimierska  <https://orcid.org/0000-0002-6227-9452>

Magdalena Kasprowicz  <https://orcid.org/0000-0002-2271-7737>

References

- Aggarwal S, Brooks D M, Kang Y, Linden P K and Patzer J F 2nd 2008 Noninvasive monitoring of cerebral perfusion pressure in patients with acute liver failure using transcranial Doppler ultrasonography *Liver Transplantation* **14** 1048–57
- Balédent O, Gondry-Jouet C, Meyer M-E, De Marco G, Le Gars D, Henry-Feugas M-C and Idy-Peretti I 2004 Relationship between cerebrospinal fluid and blood dynamics in healthy volunteers and patients with communicating hydrocephalus *Investigative Radiology* **39** 45–55
- Berdyga J, Czosnyka M, Czernicki Z and Williamson M 1993 Analysis of the intracranial pressure waveform by means of spectral methods *Intracranial Pressure VIII* ed C J J Avezaat, J H M van Eijndhoven, A I R Maas and J T J Tans (Berlin, Heidelberg: Springer) 372–5
- Bishop S M and Ercole A 2018 Multi-scale peak and trough detection optimised for periodic and quasi-periodic neuroscience data *Intracranial Pressure and Neuromonitoring XVI (Acta Neurochirurgica Supplement 126)* ed T Heldt (Cham: Springer) 189–95
- Boon A J, Tans J T, Delwel E J, Egeler-Peerdeman S M, Hanlo P W, Wurzer H A, Avezaat C J, De Jong D A, Gooskens R H and Hermans J 1997 Dutch normal-pressure hydrocephalus study: prediction of outcome after shunting by resistance to outflow of cerebrospinal fluid *Journal of Neurosurgery* **87** 687–93
- Børgesen S E and Gjerris F 1982 The predictive value of conductance to outflow of CSF in normal pressure hydrocephalus *Brain: a Journal of Neurology* **105** 65–86
- Cardoso E R, Rowan J O and Galbraith S 1983 Analysis of the cerebrospinal fluid pulse wave in intracranial pressure *Journal of Neurosurgery* **59** 817–21
- Carrera E, Kim D-J, Castellani G, Zweifel C, Czosnyka Z, Kasprovicz M, Smielewski P, Pickard J D and Czosnyka M 2010 What shapes pulse amplitude of intracranial pressure? *Journal of Neurotrauma* **27** 317–24
- Chopp M and Portnoy H D 1980 Systems analysis of intracranial pressure: comparison with volume-pressure test and CSF-pulse amplitude analysis *Journal of Neurosurgery* **53** 516–27
- Christensen L and Børgesen S E 1989 Single pulse pressure wave analysis by fast Fourier transformation *Neurological Research* **11** 197–200
- Contant C F Jr, Robertson C S, Crouch J, Gopinath S P, Narayan R K and Grossman R G 1995 Intracranial pressure waveform indices in transient and refractory intracranial hypertension *Journal of Neuroscience Methods* **57** 15–25
- Czosnyka M, Richards H K, Czosnyka Z, Piechnik S and Pickard J D 1999 Vascular components of cerebrospinal fluid compensation *Journal of Neurosurgery* **90** 752–9
- Czosnyka M, Whitehouse H, Smielewski P, Simac S and Pickard J D 1996 Testing of cerebrospinal compensatory reserve in shunted and non-shunted patients: a guide to interpretation based on an observational study *Journal of Neurology, Neurosurgery and Psychiatry* **60** 549–58
- Czosnyka M, Wollk-Laniewski P, Batorski L and Zaworski W 1988 Analysis of intracranial pressure waveform during infusion test *Acta Neurochirurgica* **93** 140–5
- de Riva N, Budohoski K P, Smielewski P, Kasprovicz M, Zweifel C, Steiner L A, Reinhard M, Fabregas N, Pickard J D and Czosnyka M 2012 Transcranial Doppler pulsatility index: what it is and what it isn't *Neurocritical Care* **17** 58–66
- Elixmann I M, Hansinger J, Goffin C, Antes S, Radermacher K and Leonhardt S 2012 Single pulse analysis of intracranial pressure for a hydrocephalus implant 2012 *Annual International Conference of the IEEE Engineering in Medicine and Biology Society (San Diego, CA, USA)* (IEEE) 3939–42
- Ellis T, McNames J and Goldstein B 2006 Residual pulse morphology visualization and analysis in pressure signals 2005 *IEEE Engineering in Medicine and Biology 27th Annual Conference (Shanghai, China)* (IEEE) 3966–9
- Fan J-Y, Kirkness C, Vicini P, Burr R and Mitchell P 2008 Intracranial pressure waveform morphology and intracranial adaptive capacity *American Journal of Critical Care* **17** 545–54
- Germon K 1988 Interpretation of ICP pulse waves to determine intracerebral compliance *The Journal of Neuroscience Nursing: Journal of the American Association of Neuroscience Nurses* **20** 344–51
- Heldt T, Zoerle T, Teichmann D and Stocchetti N 2019 Intracranial pressure and intracranial elastance monitoring in neurocritical care *Annual Review of Biomedical Engineering* **21** 523–49
- Hu X, Xu P, Scalzo F, Vespa P and Bergsneider M 2008 Morphological clustering and analysis of continuous intracranial pressure *IEEE Transactions on Biomedical Engineering* **56** 696–705
- Katzman R and Hussey F 1970 A simple constant-infusion manometric test for measurement of CSF absorption: I. Rationale and method *Neurology* **20** 534–534
- Kazimierska A, Kasprovicz M, Czosnyka M, Placek M M, Balédent O, Smielewski P and Czosnyka Z 2021 Compliance of the cerebrospinal space: comparison of three methods *Acta Neurochirurgica* **163** 1979–89
- Khan K S and Wiersema U F 2020 Transcranial Doppler waveform changes due to increased cerebrovascular resistance and raised intracranial pressure in a patient with cirrhosis: a difference in shapes, not in numbers *Journal of Clinical Ultrasound* **48** 59–63
- Kim D-J, Czosnyka M, Kim H, Balédent O, Smielewski P, Garnett M R and Czosnyka Z 2015 Phase-shift between arterial flow and ICP pulse during infusion test *Acta Neurochirurgica* **157** 633–8
- Lawley J S et al 2019 Safety, hemodynamic effects, and detection of acute xenon inhalation: rationale for banning xenon from sport *Journal of Applied Physiology* **127** 1511–8
- Little A S, Zabramski J M, Peterson M, Goslar P W, Wait S D, Albuquerque F C, McDougall C G and Spetzler R F 2008 Ventriculoperitoneal shunting after aneurysmal subarachnoid hemorrhage: analysis of the indications, complications, and outcome with a focus on patients with borderline ventriculomegaly *Neurosurgery* **62** 618–27
- Marmarou A, Foda M A A-E, Bandoh K, Yoshihara M, Yamamoto T, Tsuji O, Zasler N, Ward J D and Young H F 1996 Posttraumatic ventriculomegaly: hydrocephalus or atrophy? A new approach for diagnosis using CSF dynamics *Journal of Neurosurgery* **85** 1026–35
- Marmarou A, Shulman K and Rosende R M 1978 A nonlinear analysis of the cerebrospinal fluid system and intracranial pressure dynamics *Journal of Neurosurgery* **48** 332–44
- Mataczynski C, Kazimierska A, Uryga A, Burzynska M, Rusiecki A and Kasprovicz M 2021 End-to-end automatic morphological classification of intracranial pressure pulse waveforms using deep learning *IEEE Journal of Biomedical and Health Informatics* **In Press** 1–11
- May J O and Looney S W 2020 Sample size charts for Spearman and Kendall coefficients *Journal of Biometrics and Biostatistics* **11** 1–7
- Meese W, Kluge W, Grumme T and Hopfenmuller W 1980 CT evaluation of the CSF spaces of healthy persons *Neuroradiology* **19** 131–6
- Megjhani M et al 2019 An active learning framework for enhancing identification of non-artifactual intracranial pressure waveforms *Physiological Measurement* **40** 015002
- Nucci C G, De Bonis P, Mangiola A, Santini P, Sciandrone M, Risi A and Anile C 2016 Intracranial pressure wave morphological classification: automated analysis and clinical validation *Acta Neurochirurgica* **158** 581–8

- Plougmann J, Astrup J, Pedersen J and Gyldensted C 1994 Effect of stable xenon inhalation on intracranial pressure during measurement of cerebral blood flow in head injury *Journal of Neurosurgery* **81** 822–8
- Portnoy H D and Chopp M 1981 Cerebrospinal fluid pulse wave form analysis during hypercapnia and hypoxia *Neurosurgery* **9** 14–27
- Purkayastha S and Sorond F 2012 Transcranial Doppler ultrasound: technique and application *Seminars in Neurology* **32** 411–20
- Robertson C S, Narayan R K, Contant C F, Grossman R G, Gokaslan Z L, Pahwa R, Caram P, Bray R S and Sherwood A M 1989 Clinical experience with a continuous monitor of intracranial compliance *Journal of Neurosurgery* **71** 673–80
- Smielewski P, Czosnyka Z, Kasprowicz M, Pickard J D and Czosnyka M 2012 ICM+: a versatile software for assessment of CSF dynamics *Intracranial Pressure and Brain Monitoring XIV (Acta Neurochirurgica Supplement 114)* ed M Schuhmann and M Czosnyka (Vienna: Springer) 75–9
- Tans J T J and Boon A J W 2002 How to select patients with normal pressure hydrocephalus for shunting *Intracranial Pressure and Brain Biochemical Monitoring (Acta Neurochirurgica Supplement 81)* ed M Czosnyka, J D Pickard, P J Kirkpatrick, P Smielewski and P Hutchinson (Vienna: Springer) 3–5
- Thorpe S G, Thibeault C M, Canac N, Jalaleddini K, Dorn A, Wilk S J, Devlin T, Scalzo F and Hamilton R B 2020 Toward automated classification of pathological transcranial Doppler waveform morphology via spectral clustering *PLoS One* **15** e0228642